Progress in Nuclear Energy 78 (2015) 196–200

Contents lists available at ScienceDirect

Progress in Nuclear Energy

journal homepage: www.elsevier.com/locate/pnucene

Prediction of CHF in vertical heated tubes based on CFD methodology

Rui Zhang, Tenglong Cong, Wenxi Tian, Suizheng Qiu, Guanghui Su*

School of Nuclear Science and Technology, State Key Laboratory of Multiphase Flow in Power Engineering, Xi'an Jiaotong University, Xi'an 710049, China

ARTICLE INFO

Article history:
Received 13 August 2014
Received in revised form
29 September 2014
Accepted 6 October 2014
Available online 21 October 2014

Keywords:
Critical heat flux (CHF)
Departure from nucleate boiling (DNB)
Subcooled boiling
Critical heat flux model

ABSTRACT

Two-fluid model coupled with improved RPI wall boiling model (CHF model) was employed to investigate the departure from nuclear boiling (DNB) phenomena in vertical pipes under extremely high heat flux by using FLUENT 14.5 code. The distributions of temperature before and after DNB and the critical heat fluxes (CHF) at corresponding DNB points were obtained. The maximum deviation of predicted CHFs with experimental data was less than 15.0%. The results proved that two-fluid model coupled with CHF model was qualified to predict CHF accurately. This work can be referred when one predicts CHF in complicated geometry by CFD methodology.

1. Introduction

Subcooled boiling denotes the physical phenomenon where the wall temperature is high enough to motivate boiling at the wall even though the bulk average temperature is below the saturation value. More and more attention has been attracted by subcooled boiling for its great improvement on the capacity of heat transfer for pipes compared with single phase forced convection. Hence subcooled boiling is widely used in industrial applications. Subcooled boiling may also occur in some equipment in nuclear power plant, such as the reactor core. However, heat transfer ability can not always be enhanced by subcooled boiling with increasing wall heat flux, since heat transfer deterioration may occur when heat flux reach a certain value, named critical heat flux (CHF). This phenomenon of heat transfer deterioration is defined as departure from nucleate boiling (DNB). When DNB occurs, heated wall temperature may increase hundreds of kelvin. This temperature increase can result in tube melt or destruction. Thus, it is essential to predict CHF accurately and to maintain heat flux at wall below CHF.

In the past decades, CHF was investigated by experiments and empirical or semi-empirical correlations developed based on experiments in general. These correlations can predict CHF within the experimental data range with average deviation less than 25%, such as W-3 correlation. However, the usage of all these correlations was limited by application scope, i.e., range of experiment data. Besides, correlations can only be used for certain geometry since the experiments were executed in corresponding geometry. For complicated geometry, correlations developed based on experimental data from simple geometry, such as circular or rectangular channel, were not suitable. For this situation, researchers have to do experiments to investigate the CHF. However, it is difficult to measure temperature distribution in a complicated geometry, such as fuel assembly with grids.

With further understanding of the mechanism of subcooled boiling and DNB, it is possible for researchers to investigate subcooled boiling and DNB and predict CHF by numerical methodology. Chen et al. (Chen et al., 2009) simulated the upward subcooled boiling flow of R113 in vertical tube by CFX code with user defined FORTRAN and investigated the influences of physical properties, bubble diameter and variable saturation temperature on the predicted results. Ose and Kunugi (Ose and Kunugi, 2011) developed a numerical solution for pool subcooled boiling simulation. Krepper et al. (Krepper et al., 2007; Krepper and Rzehak, 2011; Krepper et al., 2013) predicted subcooled boiling process in vertical heated tubes with water and R12 as work fluid based on PRI wall boiling models.

In this paper, an improved wall boiling model based on the RPI wall boiling model (Kurul and Podowski, 1991) was employed to study the DNB phenomena and to predict CHF in vertical pipes. The conservation equations as well as auxiliary equations were solved by CFD code FLUENT 14.5. Moreover, the calculated CHF data were compared with experiment data of Celata et al. (1993) to validate the CHF model. The comparison between calculated and experimental CHF data shown that the CHF model was potential to predict the CHF in fuel assembly.

* Corresponding author. Tel./fax: +86 29 82663401.
E-mail address: ghsu@mail.xjtu.edu.cn (G. Su).

http://dx.doi.org/10.1016/j.pnucene.2014.10.001
0149-1970/

Nomenclature

A_b	proportion of bubbles at heated wall
c_p	Specific heat at constant pressure
d_{bw}	Bubble departure diameter
f	bubble departure frequency
F_D	drag force
$F_{L,i}$	lift force
F_{td}	turbulence dispersion force
F_{vm}	virtual mass force
F_{wl}	wall lubrication force
g	gravity
h	enthalpy
h_{fg}	latent of vaporization
h_{sl}	volumetric heat transfer coefficient
k_l	liquid conductivity
m	mass
N_w	nucleate site density
p	pressure
$\vec{q}$	heat flux
q_C	single-phase convective heat flux
q_E	the evaporate heat flux
q_Q	quenching heat flux
S	Source term
T	temperature
t	time
v	velocity
V_d	bubble volume

Greek symbols

α	void fraction
ρ	density
$\bar{\bar{\tau}}_i$	stress tensor

Subscripts

g	gas
i	liquid or gas Phase
l	liquid
sat	saturation
sub	subcooled fluid
w	wall

2. Mathematical and physical models

Eulerian multiphase model as well as interphase mass, momentum and energy transfer models is employed to consider the non-equilibrium between two phases. All these interphase interactions are calculated based on the interfacial area density model. CHF mechanism is modeled by the improved wall boiling model (i.e., the CHF model). The governing equations and auxiliary equations are given in the following of this part.

2.1. Conservation equation

Conservation equations of Eulerian two-phase model include mass, momentum and energy equations for each phase, i.e.,

mass equation

$$\frac{\partial}{\partial t}(\alpha_i\rho_i) + \nabla\cdot(\alpha_i\rho_i\vec{v}_i) = S_i + \dot{m}_{ji} - \dot{m}_{ij} \tag{1}$$

momentum equation

$$\frac{\partial(\alpha_i\rho_i\vec{v}_i)}{\partial t} + \nabla\cdot(\alpha_i\rho_i\vec{v}_i\vec{v}_i) = -\alpha_i\nabla p + \nabla\cdot\bar{\bar{\tau}}_i + \alpha_i\rho_i\vec{g} + \dot{m}_{ji}\vec{v}_j - \dot{m}_{ij}\vec{v}_i + \vec{F}_{D,i} + \vec{F}_{L,i} + \vec{F}_{wl,i} + \vec{F}_{td,i} + \vec{F}_{vm,i} \tag{2}$$

energy equation

$$\frac{\partial}{\partial t}(\alpha_i\rho_i h_i) + \nabla\cdot(\alpha_i\rho_i\vec{v}_i h_i) = \alpha_i\frac{\partial p_i}{\partial t} - \nabla\cdot\vec{q}_i + S_i + Q_{ij} + \dot{m}_{ji}h_j - \dot{m}_{ij}h_i \tag{3}$$

where α_i, ρ_i, $\vec{v}_i$, S_i, p_i, $\bar{\bar{\tau}}_i$, h_i and $\vec{q}_i$ denote the volume of fraction, density, velocity, source term, pressure, stress tensor, specific enthalpy and heat flux for i phase, respectively. $\dot{m}_{ji}$ and Q_{ji} are the mass and energy transfer from jth to ith phase, separately. $\vec{F}_{D,i}$, $\vec{F}_{L,i}$, $\vec{F}_{wl,i}$, $\vec{F}_{td,i}$ and $\vec{F}_{vm,i}$ are the drag force, lift force, wall lubrication force, turbulence dispersion force and virtual mass force, respectively.

2.2. Improved wall boiling model – CHF model

According to the CHF model employed in this work, the total heat flux from heated wall to the fluid is divided into two components, heat flux transferred to liquid phase (q_f) and heat flux transferred to vapor phase (q_g). Among these two components, heat flux to liquid phase is partitioned into three parts, the single-phase convective heat flux, q_c, the evaporate heat flux, q_e, and the wall quenching heat flux, q_q. Thus, the total heat flux can be expressed as.

$$q_w = f\left(\alpha_f\right)\left(q_c + q_e + q_q\right) + \left(1 - f\left(\alpha_f\right)\right)q_g \tag{4}$$

where $f(\alpha_f)$ is the area fraction of heated wall dominated by liquid phase, including the wall area fractions covered by convective liquid phase and by nucleating bubbles; $(1-f(\alpha_f))$ is the area fraction of heated wall covered by single phase vapor; $f(\alpha_f)$ is estimated by Ioilev model (Ioilev et al., 2007).

$$f\left(\alpha_f\right) = 1 - \max\left(0, \min\left\{1, \frac{\alpha_g - \alpha_{g,1}}{\alpha_{g,2} - \alpha_{g,1}}\right\}\right) \tag{5}$$

The four heat fluxes can be expressed as,

$$q_C = h_f(T_w - T_l)(1 - A_b) \tag{6}$$

$$q_e = V_d N_w \rho_g h_{fg} f \tag{7}$$

$$q_q = \frac{2\sqrt{k_l\rho_l c_{p,l} f}}{\sqrt{\pi}}(T_w - T_l) \tag{8}$$

$$q_g = h_g\left(T_w - T_g\right) \tag{9}$$

where h_f and h_g denotes the single phase turbulent heat transfer coefficient of liquid and vapor phase, respectively; T_w, T_l and T_g are the temperature of heated wall, liquid and fluid, respectively; ρ_l and ρ_g are the density of liquid and vapor phase, respectively; h_{fg} is the latent heat of evaporation; V_d is the volume of the bubbles based on

the bubble departure diameter; $c_{p,l}$ and k_l are the specific heat and conductivity of liquid phase, respectively. A_b is the proportion of heated wall covered by nucleating bubbles, while $(1 - A_b)$ is the proportion of heated wall covered by single phase liquid; A_b is estimated by

$$A_b = \min\left(1, K\frac{N_w \pi d_{bw}^2}{4}\right) \tag{10}$$

where d_{bw} is the bubble departure diameter, given by Tolubinsky model (Tolubinsky and Kostanchuk, 1970),

$$d_{bw} = \min\left(0.0006 \cdot e^{\left(-\frac{\Delta T_{sub}}{45.0}\right)}, 0.0014\right) \tag{11}$$

and K is an empirical constant estimated by Del Valle and Kenning equation (Del Valle and Kenning, 1985)

$$K = 4.8 \exp\left(-\frac{\rho_l c_{p,l}(T_w - T_l)}{80\rho_g h_{fg}}\right) \tag{12}$$

N_w is the active nucleate site density, given by Lemmert and Chawla (1977) model.

$$N_w = 210^{1.805}(T_w - T_{sat})^{1.805} \tag{13}$$

where T_{sat} is the saturated temperature. f is the frequency of bubble departure, given by Cole correlation (Cole, 1960),

$$f = \frac{1}{T} = \sqrt{\frac{4g(\rho_l - \rho_g)}{3d_{bw}\rho_l}} \tag{14}$$

where g is the gravitational acceleration.

2.3. Interfacial heat transfer

Interfacial heat transfer includes the heat transfer from liquid to vapor phase at the near wall region and the heat transfer between vapor and liquid phases in the subcooled bulk. Heat transferred to vapor is calculated by

$$\dot{q}_{vt} = \frac{\alpha_v \rho_v C_{p,v}}{\delta t}\left(T_{sat} - T_v\right) \tag{15}$$

where δt is the time scale set to a default value of 0.05 according to (Laviéville et al., 2005).

When the bubble departs from the heated wall and moves towards the subcooled mainstream, the heat transferred from the vapor to the liquid is calculated as,

$$\dot{q}_{lt} = h_{sl}(T_{sat} - T_l) \tag{16}$$

where h_{sl} is the volumetric heat transfer coefficient calculated by Ranz-Marshall model (1952).

2.4. Interfacial mass transfer

For subcooled boiling, the process of mass transfer consists of these two aspects: liquid evaporation near the wall and liquid evaporation or vapor condensation in bulk flow. The evaporation mass flux in near wall cells can be calculated on the basis of evaporation heat flux,

$$\dot{m}_E = \frac{\dot{q}_E}{h_{fg} + C_{p,l}\Delta T_{sub}} \tag{17}$$

Mass transfer rate in subcooled region depends on the difference of temperature between each phase. When the liquid is subcooled, steam condensates; when the liquid is superheated, liquid evaporates. The interfacial mass transfer rate can be written as,

$$\dot{m} = \dot{m}_{lt} + \dot{m}_{vt} = \frac{\dot{q}_{lt} + \dot{q}_{vt}}{h_{fg}} \tag{18}$$

2.5. Interfacial momentum transfer

The interfacial momentum transfer between liquid and vapor phases includes the drag force, lift force, wall lubrication force, turbulent dispersion force and virtual mass force, which are given in detail.

The frag force, which is flow region dependent, is modeled by.

$$\vec{F}_D = \frac{C_D \mu_l A_{if} Re}{8 d_g}\left(\vec{v}_g - \vec{v}_l\right) \tag{19}$$

where C_D is the drag force coefficient, estimated by Ishii model (Ishii, 1990); μ_l is the viscosity of liquid phase; A_{if} is the interfacial area concentration; Re is the relative Reynolds number based on the average bubble diameter; d_g is the average bubble diameter.

The lift force, presenting the force act on vapor phase due to velocity gradients in the liquid phase, is calculated by

$$\vec{F}_L = -C_L \rho_l \alpha_g\left(\vec{v}_l - \vec{v}_g\right) \times (\nabla \times \vec{v}_l) \tag{20}$$

where C_L is the lift force coefficient given by Moraga model (Moraga et al., 1999).

The wall lubrication force, used to push the vapor phase away from the walls to bulk flow, is defined as

$$\vec{F}_{wl} = C_{wl}\rho_l \alpha_g \left|\vec{v}_{l,z} - \vec{v}_{g,z}\right|^2 \vec{n}_w \tag{21}$$

where C_{wl} is the wall lubrication coefficient given by Antal model (Antal et al., 1991); $\vec{v}_{l,z}$ and $\vec{v}_{g,z}$ are the velocity component tangential to the wall surface of liquid and vapor phase, respectively; $\vec{n}_w$ is the unit normal pointing away from the wall.

The turbulent dispersion force, including the effects of interphase turbulent momentum transfer, play a key role in take the vapor away from the near wall region to the subcooled bulk. It can be calculated by Burns model (Burns et al., 2004).

$$\vec{F}_{td} = C_{TD}\frac{C_D \mu_l \mu_{t,l} A_{if} Re}{8 d_g \rho_l \sigma_{lg}}\left(\frac{\nabla \alpha_g}{\alpha_g} - \frac{\nabla \alpha_l}{\alpha_l}\right) \tag{22}$$

where $C_{TD} = 1$ and $\sigma_{lg} = 0.9$.

The virtual mass force, playing a role when vapor phase accelerates relative to liquid phase, is defined by.

$$\vec{F}_{vm} = 0.5\alpha_g \rho_l\left(\frac{\partial \vec{v}_l}{\partial t} + (\vec{v}_l \cdot \nabla)\vec{v}_l - \left(\frac{\partial \vec{v}_g}{\partial t} + (\vec{v}_g \cdot \nabla)\vec{v}_g\right)\right) \tag{23}$$

2.6. Turbulence model

After comparing calculated results with experimental data of subcooled boiling and CHF, realizable k-ε turbulence model and enhanced wall function were employed to solve the turbulent parameters.

3. Grid model, boundary conditions and numerical method

The benchmark data of this work were obtained from CHF experiment in vertical upward-flow pipe published by Celata et al. (1993). In Celata et al.'s work, stainless steel tubes of 2.5 mm inner diameter and 100 mm length were employed to find the CHF in subcooled flow boiling with extremely high heat flux. Similar to the experiment, a 100 mm entrance section was preceded and followed by the test section. To simplify the calculation, a quarter of the test pipe was selected as the calculated domain. The schematic diagrams of geometry and boundary conditions are given in Fig. 1. To solve the governing equations as well as auxiliary equations, COUPLED algorithm in FLUENT code was used. The gradient was discretized by least squares cell based method. All other governing equations were discretized by QUICK method. After checking the grid independence by using four sets of grid containing 12,000, 26,400, 39,000 and 57,600 meshes respectively, we employ the grid scheme with 39,000 meshes as the grid independent grid for further calculation. The near wall cell $Y+$ for all the calculation based on this grid located in the range of 28.3–63.6.

4. Results and discussion

Similar to the experimental procedure, we increased the wall heat flux at heated wall by step of 0.5 MW/m^2 at first and then changed the step to 0.1 MW/m^2 after the CHF was approached (70% of the CHF estimated by Gunther correlation). Wall temperature increased with increasing the heat flux by little temperature step at first, and then it jumped dramatically when DNB occurred. A typical curve of maximum wall temperature with iteration was shown in Fig. 2. As can be seen, heat flux of 0.5 WM/m^2 was set at the initial phase of calculation; after convergence (300 iteration for each heat flux step), wall heat flux was increased by 0.5 or 0.1 MW/m^2 till the DNB phenomena were detected. The wall temperature distributions along the axial direction before and after DNB were given in Fig. 3. As can be noted, wall temperature ascended gradually when the heat flux was low than CHF; however, when the heat flux reached CHF, wall temperature shot up rapidly at a certain point where DNB occurred.

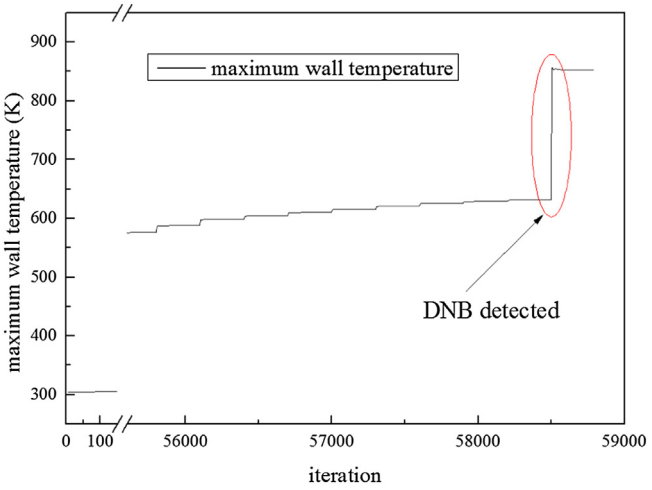

Fig. 2. Maximum wall temperature with increasing wall heat flux.

At last, we calculated 26 sets of Celata et al.'s experimental data and obtained the corresponding CHF data. The comparison of calculated CHF data with experimental data was given in Fig. 4. As shown in this figure, the predicted results agreed quite well with experimental ones with deviations less than 15.0%. The mean absolute relative error of the calculated CHF (estimated by $\frac{1}{N}\sum_{i=1}^{N}\left|\frac{CHF_{exp,i}-CHF_{cal,i}}{CHF_{exp,i}}\right|$) was 7.1%.

5. Conclusions

In this study, CHF model based on RPI wall boiling model was employed to investigate the DNB phenomena and predict CHF in vertical pipe. The deviations between predicted CHF and experimental CHF were less than 15.0% for most data. The mean absolute relative error of calculated CHF was 7.1%. The results proved that the

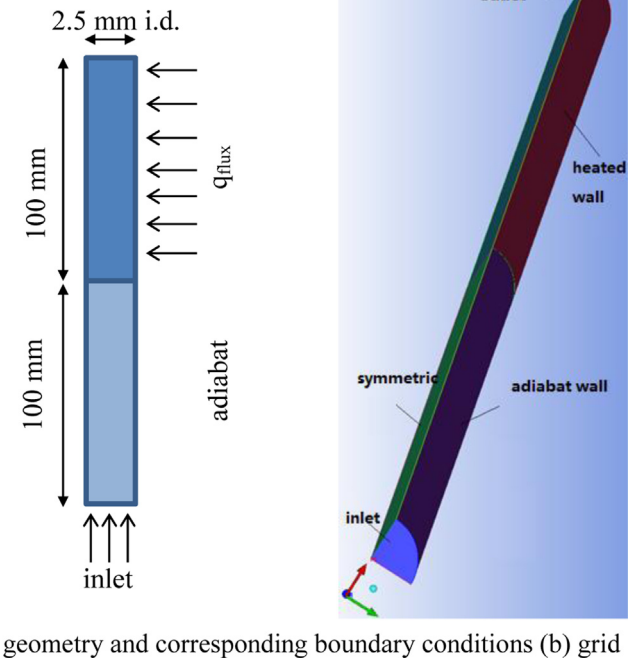

(a) geometry and corresponding boundary conditions (b) grid

Fig. 1. Geometry, boundary and grid.

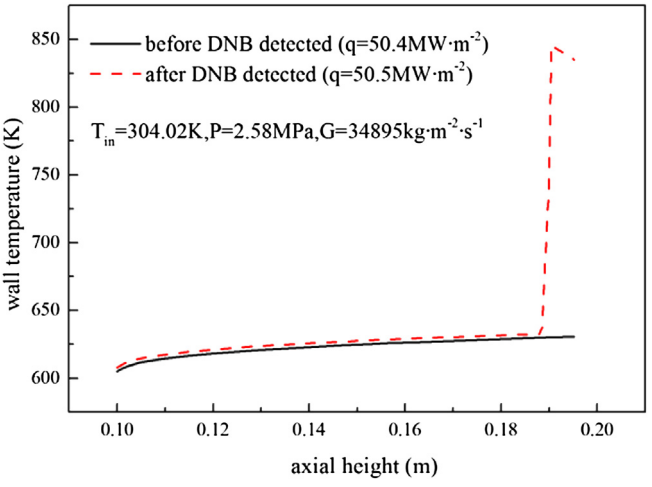

Fig. 3. Wall temperature along the axial direction.

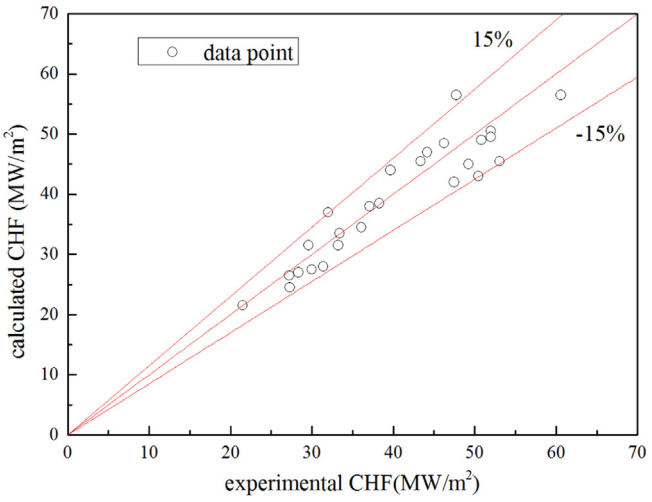

Fig. 4. Comparison of calculated CHF with experimental CHF.

CHF model utilized in the current work was qualified to predicted CHF. This CHF model is potential to predict CHF in fuel assembly in reactor core.

Acknowledgments

This work is supported by the New Century Program Foundation for Excellent Talents from the Ministry of Education of China (No. NCET-11-0430) and the National Science Fund for Distinguished Young Scholars in China (No. 11125522), which are gratefully acknowledged.

References

Antal, S., Lahey Jr., R., Flaherty, J., 1991. Analysis of phase distribution in fully developed laminar bubbly two-phase flow. Int. J. Multiph. Flow 17, 635–652.
Burns, A.D., Frank, T., Hamill, I., Shi, J.-M., 2004. The Favre Averaged Drag Model for Turbulent Dispersion in Eulerian Multi-phase flows, 5th International Conference on Multiphase Flow, ICMF.
Celata, G.P., Cumo, M., Mariani, A., 1993. Burnout in highly subcooled water flow boiling in small diameter tubes. Int. J. Heat Mass Transf. 36, 1269–1285.
Chen, E., Li, Y., Cheng, X., 2009. CFD simulation of upward subcooled boiling flow of refrigerant-113 using the two-fluid model. Appl. Therm. Eng. 29, 2508–2517.
Cole, R., 1960. A photographic study of pool boiling in the region of the critical heat flux. AIChE J. 6, 533–538.
Del Valle, V.H., Kenning, D., 1985. Subcooled flow boiling at high heat flux. Int. J. Heat Mass Transf. 28, 1907–1920.
Ioilev, A., Samigulin, M., Ustinenko, V., Kucherova, P., Tentner, A., Lo, S., Splawski, A., 2007. Advances in the modeling of cladding heat transfer and critical heat flux in boiling water reactor fuel assemblies. In: Proc. 12th International Topical Meeting on Nuclear Reactor Thermal Hydraulics (NURETH-12), Pittsburgh, Pennsylvania, USA.
Ishii, M., 1990. Two-fluid model for two-phase flow. Multiph. Sci. Technol. 5.
Krepper, E., Končar, B., Egorov, Y., 2007. CFD modelling of subcooled boiling—Concept, validation and application to fuel assembly design. Nucl. Eng. Des. 237, 716–731.
Krepper, E., Rzehak, R., 2011. CFD for subcooled flow boiling: simulation of DEBORA experiments. Nucl. Eng. Des. 241, 3851–3866.
Krepper, E., Rzehak, R., Lifante, C., Frank, T., 2013. CFD for subcooled flow boiling: Coupling wall boiling and population balance models. Nucl. Eng. Des. 255, 330–346.
Kurul, N., Podowski, M.Z., 1991. On the Modeling of Multidimensional Effects in Boiling Channels, Proceedings of the 27th National Heat Transfer Conference, Minneapolis, Minn, USA.
Laviéville, J., Quemerais, E., Mimouni, S., Boucker, M., Mechitoua, N., 2005. NEPTUNE CFD V1. 0 Theory Manual. EDF, France.
Lemmert, M., Chawla, J., 1977. Influence of flow velocity on surface boiling heat transfer coefficient. Heat Transf. Boil. 237, 247.
Moraga, F., Bonetto, F., Lahey, R., 1999. Lateral forces on spheres in turbulent uniform shear flow. Int. J. Multiph. Flow 25, 1321–1372.
Ose, Y., Kunugi, T., 2011. Development of A Boiling and condensation model on subcooled boiling phenomena. Energy Procedia 9, 605–618.
Ranz, W., Marshall, W., 1952. Evaporation from drops. Chem. Eng. Prog. 48, 141–146.
Tolubinsky, V., Kostanchuk, D., 1970. Vapour bubbles growth rate and heat transfer intensity at subcooled water boiling. Heat. Transf. 1–5.